DALTON

Solvent extraction of metal ions from nitric acid solution using *N*,*N*′-substituted malonamides. Experimental and crystallographic evidence for two mechanisms of extraction, metal complexation and ion-pair formation†

Gabriel Y. S. Chan,[a] Michael G. B. Drew,*[,a] Michael J. Hudson,*[,a] Peter B. Iveson,[a] Jan-Olov Liljenzin,[b] Mats Skålberg,[b] Lena Spjuth[b] and Charles Madic[c]

[a] *Department of Chemistry, University of Reading, PO Box 224, Whiteknights, Berkshire RG6 6AD, UK*
[b] *Department of Nuclear Chemistry, Chalmers University of Technology, S-412 96 Göteborg, Sweden*
[c] *Commissariat à l'Energie Atomique, Bat. 399, B.P. 171, 30207 Bagnols-sur-Cèze, Cedex, France*

The solvent extraction of actinides including Am^{III} and Cm^{III} together with some trivalent lanthanides from nitric acid solutions by two newly synthesized malonamides, *N*,*N*′-dimethyl-*N*,*N*′-diphenyltetradecylmalonamide (dmptdma) and *N*,*N*′-dicyclohexyl-*N*,*N*′-dimethyltetradecylmalonamide (dcmtdma) has been investigated and compared with data for the reference malonamide, *N*,*N*′-dibutyl-*N*,*N*′-dimethyloctadecylmalonamide (dbmocma). The dependence of the extraction on the nitric acid and malonamide concentrations together with the probable molecular structure of the extraction species from nitric acid solution suggests that there are two principal mechanisms of extraction. For low nitric acid concentrations (up to 1 mol dm^{-3}) a co-ordinative mechanism dominates for the extraction of metal cations, whereas at higher nitric acid concentrations (1–14 mol dm^{-3}) an ion-pair mechanism involving the mono- or di-protonated malonamide and the metal anions $[M(NO_3)_4]^-$ or $[M(NO_3)_5]^{2-}$ appears to be more important. Crystal structures show that in the protonated, unalkylated species $Hdcmma^+$ (dcmma = *N*,*N*′-dicyclohexyl-*N*,*N*′-dimethylmalonamide) and in the chelated complexes $[Nd(NO_3)_3(dcmma)_2]$, $[Nd(NO_3)_3(H_2O)_2(dmpma)]$ and $[Yb(NO_3)_3(H_2O)(dmpma)]$ (dmpma = *N*,*N*′-dimethyl-*N*,*N*′-diphenylmalonamide) the carbonyl oxygens lie *cis* to each other suggesting that it is the *cis* form which is involved in extraction. However, crystal structures of the free unalkylated malonamides *N*,*N*′-dicyclohexyl-*N*,*N*′-diethylmalonamide and *N*,*N*′-dicyclohexyl-*N*,*N*′-diisopropylmalonamide show that the carbonyl amide groups adopt a *trans* configuration in which the carbonyl oxygens are at maximum separation. By contrast, in the crystal structure of the diphenyl derivative dmpma the carbonyl amide groups adopt a *gauche* configuration with an O=C · · · C=O torsion angle of 57.2°. Conformational analysis confirms that the differences in these structures reflect the differences between the lowest-energy gas-phase conformations and are not caused by packing effects.

One of the aims in nuclear reprocessing is the conversion or transmutation of the long-lived minor actinides such as americium into short-lived isotopes by irradiation with neutrons.[1,2] In order to achieve this transmutation it is necessary to separate the trivalent minor actinides from the trivalent lanthanides by solvent extraction because otherwise the lanthanides absorb neutrons effectively and hence prevent neutron capture by the transmutable actinides.[3,4] One option is to coextract the trivalent actinides and lanthanides from the remaining aqueous waste prior to their separation from each other. Malonamides of the type $(R^1R^2NCO)_2CHR^3$ have been suggested as possible coextractants,[5] instead of the traditional tributyl phosphate,[6,7] $(BuO)_3PO$ or (*N*,*N*-diisobutylcarbamoylmethyl)octyl(phenyl)-phosphine oxide.[8,9] The latter are phosphorus-containing extractants which ultimately create undesirable waste even after incineration. Malonamides, on the other hand, contain only the elements carbon, oxygen, hydrogen and nitrogen and hence are completely incinerable extractants. These compounds are weak bases in which the carbonyl amide groups may bind to metal ions in a chelate complex.[10] In strong acidic solutions the carbonyl amide groups may be protonated to form intramolecularly hydrogen-bonded species such as $[H(R^1R^2NCO)_2CHR^3]^+$ or $[H_2(R^1R^2NCO)_2CHR^3]^{2+}$. The chemical properties of the malonamides are influenced by the nature of the substituents on the nitrogen and the central methylene carbon atom. The choice of R^1 and R^2 groups is important. When R^1 is small (*e.g.* methyl) this limits the steric hindrance for metal-ion co-ordination; R^2 is large so that the reagents will dissolve in the organic phase.[5] Owing to the high aqueous solubility of malonamides, enhanced extraction into the organic phase can be achieved when the methylene carbon is bound to a hydrophobic group (R^3) with fourteen or more carbon atoms.[11,12] The presence of this hydrophobic group enhances the solubilities of both the free ligand and the metal complexes or ion pairs in the organic phase.

In order to rationalise some of the above observations, two new malonamides were investigated and compared with the malonamide, *N*,*N*′-dibutyl-*N*,*N*′-dimethyloctadecylmalonamide (dbmodma), which may be regarded as a reference molecule. The malonamides studied all have an *N*-methyl group plus one other group, either cyclohexyl or phenyl, attached to the nitrogen atoms. For both dbmodma and the *N*,*N*′-dicyclohexyl-*N*,*N*′-dimethyltetradecylmalonamide (dcmtdma) derivatives, the *N*-alkyl groups are rather bulky and non-planar, whereas in *N*,*N*′-dimethyl-*N*,*N*′-diphenyltetradecylmalonamide (dmdptdma) the planar phenyl group is less bulky and could lie close to the long hydrophobic alkyl chain. The bulky *N*-butyl and *N*-cyclohexyl groups possibly sterically hinder the chelation of the malonamide to the metal or the formation of

† *Non-SI units employed:* eV ≈ 1.60×10^{-19} J, hartree ≈ 4.36×10^{-18} J, cal = 4.184 J.

ion pairs. Alternatively, these malonamides can change their O=C···C=O torsion angle and the O···O distance between the carbonyl oxygen atoms; these conformational changes can be related to the extraction properties of the malonamides. *N*,*N*′-Dicyclohexyl-*N*,*N*′-dimethylmalonamide (dcmma), *N*,*N*′-dimethyl-*N*,*N*′-diphenylmalonamide (dmpma), *N*,*N*′-dicyclohexyl-*N*,*N*′-diethylmalonamide (dcema) and *N*,*N*′-dicyclohexyl-*N*,*N*′-diisopropylmalonamide (dcima) were synthesized and all shown (by NMR spectroscopy) to be conformationally flexible. In order for chelative complexation with metal ions to occur there must be a reorientation of the carbonyl groups from the *trans* to *cis* conformer. A similar rearrangement is also required once the malonamide is protonated, such that the proton is shared between the carbonyl groups of the same molecule. In order to establish the possible structures of species involved in the separation processes, the crystal structures of the free malonamides dcema, dcima and dmpma together with that of the protonated form $Hdcmma^+$ and also lanthanide complexes of the formulae $[Nd(NO_3)_3(dcmma)_2]$, $[Nd(NO_3)_3(dmpma)]\cdot 2H_2O$ and $[Yb(NO_3)_3(dmpma)]\cdot H_2O$ were determined.

Experimental

All starting chemicals for the syntheses were obtained from Aldrich and used without further purification. Microanalyses were carried out by Medac Ltd., Brunel University. Infrared spectra (4000–350 cm^{-1}) were recorded on a Perkin-Elmer 1720-X FT-IR spectrometer with an IRDM data-management system, ^1H (400 MHz) NMR spectra on a JEOL JNM-EX 400 spectrometer using either CD_3OD (unalkylated malonamides) or $CDCl_3$ (alkylated malonamides) as solvent.

Syntheses

***N*,*N*′-Tetrasubstituted malonamides.** There are a number of routes for the synthesis of malonamides. These methods include the reaction of secondary amines with acid esters (**I**), with acid anhydrides (**II**) and with acyl chlorides (**III**).[13] In this study, we adopted route (**I**) for the synthesis of *N*,*N*′-tetrasubstituted malonamides, as this was found to give the highest yields.

N,N′-*Dicyclohexyl*-N,N′-*dimethylmalonamide* (*dcmma*). This synthesis is given as an example of the method used. *N*-Methylcyclohexylamine (300 g, 2.65 mol) was initially mixed with dimethyl malonate (162 g, 1.23 mol) then heated at 75 °C for 4 h. Throughout this time the extent of reaction was monitored by Fourier-transform IR spectroscopy: the absorption at 1750 cm^{-1} due to the ester carbonyl was replaced by a band at about 1640 cm^{-1} assigned to an amide structure.[13] A white solid formed on cooling. This was washed with diethyl ether (2 × 100 cm^3) and recrystallised from ethyl acetate to give pure dcmma (216 g, 60 %). The other three *N*,*N*′-tetrasubstituted malonamides were prepared in the same way. The NMR data are shown in Table 2 and the elemental analyses and melting points in Table 1. The structural formula of each malonamide is shown in Scheme 1.

Pentaalkylmalonamides. *N*,*N*′-Dibutyl-*N*,*N*′-dimethyloctadecylmalonamide (dbmodma) was supplied by Synthelec AB, Sweden while the other pentaalkylmalonamides were synthesized at the University of Reading, UK.

N,N′-*Dicyclohexyl*-N,N′-*dimethyltetradecylmalonamide* (*dcmtdma*). This synthesis is given as an example of the method used. Sodium hydride (5.23 g of a 60% dispersion in mineral oil, 0.13 mol) was washed with light petroleum (b.p. 60–80 °C) and suspended in toluene (100 cm^3). The compound dcmma (38.22 g, 0.13 mol) was added and the mixture refluxed until hydrogen evolution had ceased (*ca.* 2 h). 1-Bromotetradecane (36.33 g, 0.13 mol) in toluene (80 cm^3) was added and the mixture refluxed until the pH became neutral (*ca.* 3 d). Toluene was removed under vacuum and a yellow solid was formed. This was dried in an oven, giving pure dcmtdma (60 g, 95%). The compound dmptdma was prepared in the same way. Again the characterisation details are summarised in Tables 1 and 2 and the structural formulae are shown in Scheme 2.

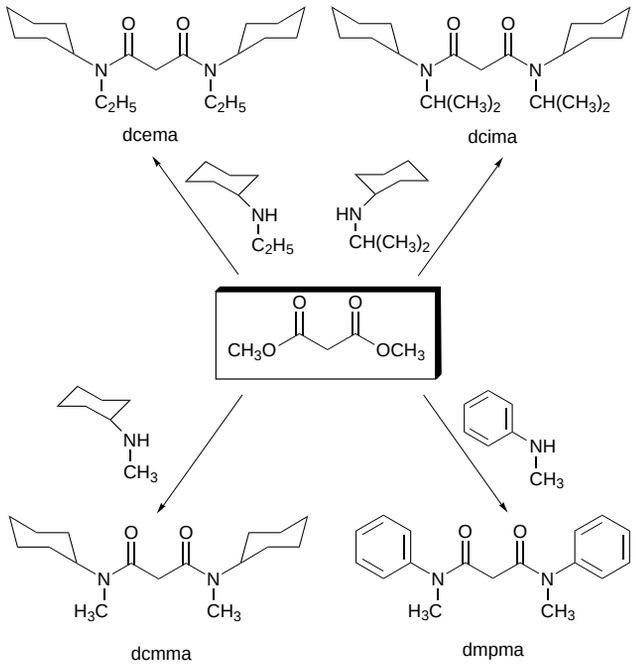

Scheme 1 Synthesis of the tetrasubstituted malonamides

Solvent extraction procedure

Nitric acid solutions were pre-equilibrated with the tracer solution before distribution ratio determination. The pentaalkylmalonamides were vigorously shaken with the aqueous phase for 5 min in order to enable equilibrium to be reached. After phase disengagement by centrifugation, aliquots from each phase were removed for radiometric analysis. The γ energies at 59.6, 122, 185 and 879 keV for ^{241}Am, ^{152}Eu, ^{235}U and ^{160}Tb respectively were measured using a solid-state HPGe detector. For the α and β emitters (*i.e.* ^{244}Cm and ^{234}Th) an LKB Wallac 1219 Rackbeta liquid scintillation counter was used. All experiments were performed with *tert*-butylbenzene as diluent. The distributions of nitric acid between the aqueous and organic phases were determined by potentiometric titration using a Mettler DL20 Compact Titrator. The titrations were performed in ethanolic media to facilitate mixing of the solutions.

Preparation of crystals

Crystals of dcema were prepared by dissolving the compound (2 g) in hot ethanol (50 cm^3) and allowing the solution to cool slowly to room temperature (yield 70–75%). Those of dcima were prepared in a similar way, except that the compound (2 g) was initially dissolved in ethanol–diethyl ether (1:1, 75 cm^3) (yield 80%). A suitable crystal of dmpma was obtained directly on slow cooling of the reaction mixture. Crystals of $Hdcmma^+$ were prepared by dissolving dcmma (0.5 g, 1.7×10^{-3} mol) in 5 mol dm^{-3} HCl (25 cm^3). Cobalt(II) chloride hexahydrate (0.54 g, 2.27×10^{-3} mol) was added to the acidic solution. The blue solution formed was then left in a thermostatted bath at 28 °C. Blue crystals were formed after 24 h (yield 70%) (Found: C, 51.3; H, 7.7; N, 7.3. $C_{34}H_{62}Cl_4CoN_4O_4$ requires C, 51.6; H, 7.9; N, 7.1%). The neodymium complex of dcmma was prepared as follows: a solution of dcmma (0.5 g, 1.7×10^{-3} mol) in

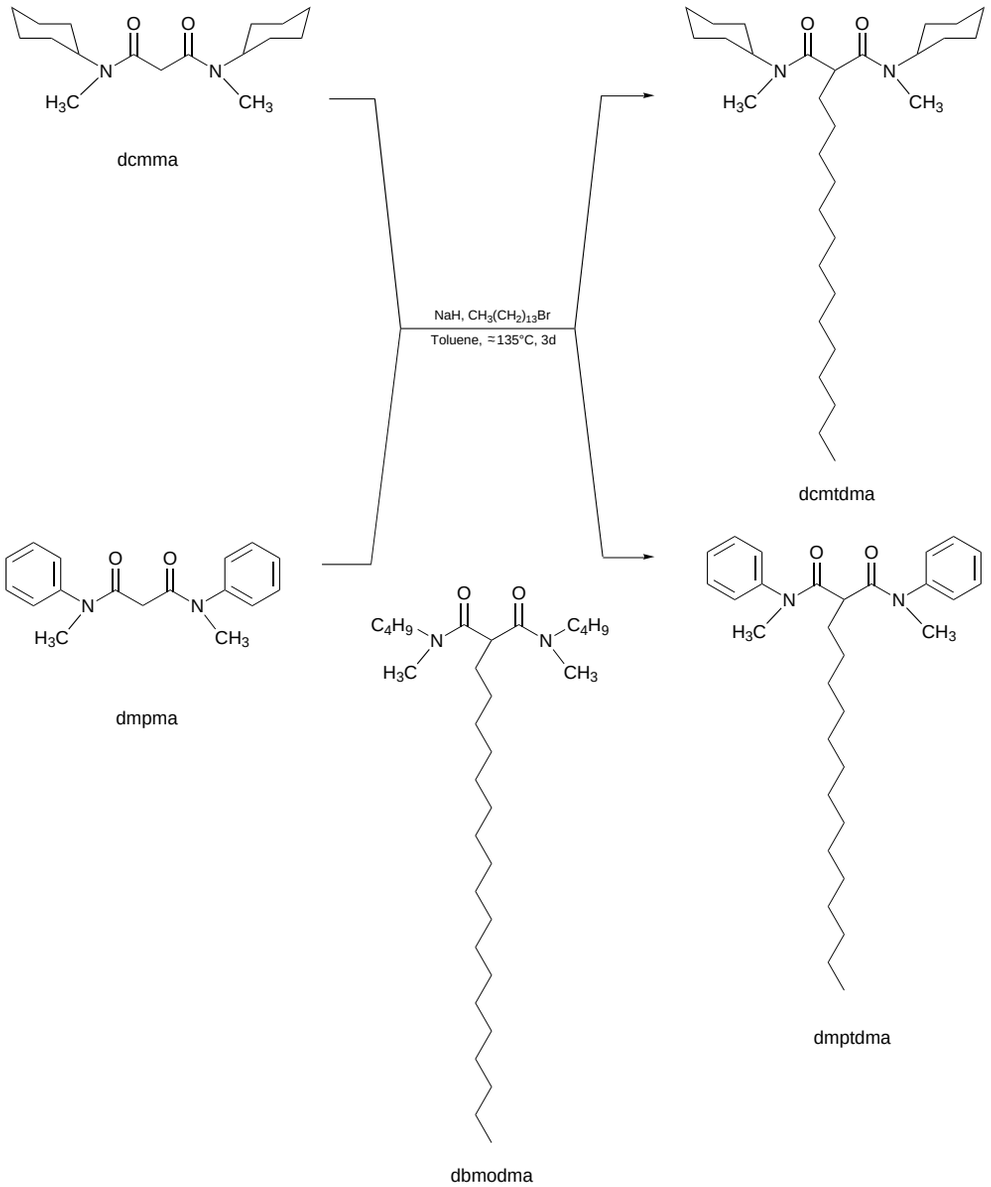

Scheme 2 Synthesis of dcmtdma and dmptdma. The structure of dbmodma is also shown

EtOH (10 cm^3) was added slowly to a stirred solution of $Nd(NO_3)_3 \cdot 6H_2O$ (1.12 g, 2.6×10^{-3} mol) in EtOH (10 cm^3). The slightly purple solution was allowed slowly to evaporate and crystals were deposited after several days at room temperature (yield 80%). The corresponding complex of dmpma was prepared by adding $Nd(NO_3)_3 \cdot 6H_2O$ (0.039 g, 0.09 mmol) dissolved in propan-2-ol (2 cm^3) to a stirred solution containing dmpma (0.05 g, 0.18 mmol) in absolute ethanol (1 cm^3) and propan-2-ol (2 cm^3). The final solution was allowed slowly to evaporate at room temperature and crystals were deposited after 2 d. These were filtered off, washed with a small amount of propan-2-ol and then dried in an oven at 90 °C for 5 h (Found: C, 30.4, H, 3.4; N, 10.7. $C_{17}H_{24}N_5NdO_{14}$ requires C, 30.6; H, 3.6; N, 10.5%). The corresponding ytterbium complex was prepared by slow addition of a propan-2-ol solution (5 cm^3) containing $Yb(NO_3)_3 \cdot 5H_2O$ (0.04 g, 0.09 mmol) to a rapidly stirred propan-2-ol solution (5 cm^3) of dmpma (0.05 g, 0.18 mmol). Crystals of $[Yb(NO_3)_3(dmpma)] \cdot H_2O$ suitable for X-ray analysis were obtained after leaving the solution to stand for 1 d at room temperature (yield 40%).

Crystallography

Crystal data are given in Table 8, together with refinement details. Data were collected at 293(2) K with Mo-Kα radiation (λ 0.710 73 Å) using the MARresearch image-plate system. Each crystal was positioned at 75 mm from the plate. Ninety-five frames were measured at 2° intervals with a counting time of 2 min. Data analysis was carried out with the XDS program.[14] The structures of the four malonamides were solved using direct methods with the SHELXS 86 program,[15] those of the three complexes by heavy-atom methods. In all seven structures the non-hydrogen atoms were refined with anisotropic thermal parameters. In all except $Hdcmma^+$ all hydrogen atoms were included in geometric positions. In $Hdcmma^+$ all hydrogen atoms bonded to carbon were included in geometric positions, but the two hydrogen atoms bonded to O(1A) and O(1B) were located in a Fourier-difference map and included with O–H constraints set at 0.95 Å. Also the $[CoCl_4]^{2-}$ anion suffered from severe anisotropy but a suitable disordered model could not be found.* In $[Nd(NO_3)_3(dmpma)] \cdot 2H_2O$ there were two molecules in the asymmetric unit. All structures were then refined using

* We also carried out a structure determination of the isomorphous copper complex: $a = 13.650(8)$, $b = 23.736(12)$, $c = 14.562(11)$ Å, $\beta = 112.42(1)°$, $U = 4361.4$ Å, monoclinic, space group $P2_1/a$. It is not of sufficient quality to report here, but contains protonated malonamide cations and $[CuCl_4]^{2-}$ anions.

Table 1 Melting points and elemental analysis data for malonamides

		Analysis (%)			Calculated		
Malonamide	M.p./ °C	C	H	N	C	H	N
dcema	121–122	70.7	10.6	8.7	70.8	10.6	8.7
dcima	147–148	71.9	10.9	7.8	71.9	10.9	7.9
dcmma	117–118	69.4	10.3	9.5	69.4	10.3	9.5
dmpma	105–106	72.2	6.5	9.9	72.3	6.4	9.9
dcmtdma	53–54	75.8	11.9	5.6	75.9	11.9	5.7
dmptdma	48–49	77.8	9.5	5.7	77.8	9.7	5.8

Table 2 Proton NMR assignments for malonamide

Malonamide	Structural formula	^{1}H NMR (δ)
dcema	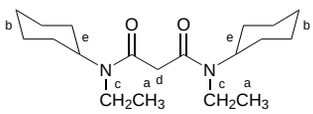	1.12–1.18 (6 H, t, a) 1.3–1.9 (20 H, m, b) 3.26–3.38 (4 H, q, c) 3.44–3.52 (2 H, s, d) 4.22–4.35 (2 H, q, e)
dcima	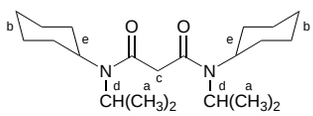	1.15–1.19 (12 H, d, a) 1.35–1.85 (20 H, m, b) 3.39–3.44 (2 H, s, c) 3.72–3.82 (2 H, h, d) 4.24–4.40 (2 H, q, e)
dcmma	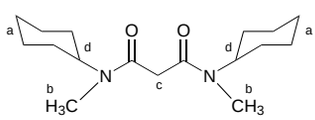	1.29–1.9 (20 H, m, a) 2.8–2.9 (6 H, s, b) 3.4–3.5 (2 H, s, c) 4.25–4.45 (2 H, q, d)
dmpma	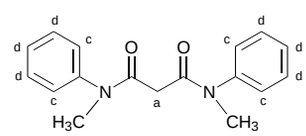	2.9–3.0 (2 H, s, a) 3.08–3.15 (6 H, s, b) 6.9–7.1 (4 H, d, c) 7.35–7.45 (6 H, t, d)
dcmtdma	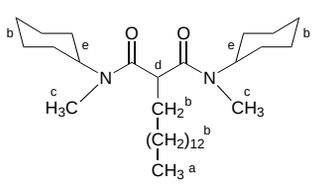	0.8–0.9 (3 H, t, a) 1.2–1.8 (46 H, m, b) 2.65–2.82 (6 H, s, c) 3.4–3.6 (1 H, t, d) 4.3–4.4 (2 H, q, e)
dmptdma	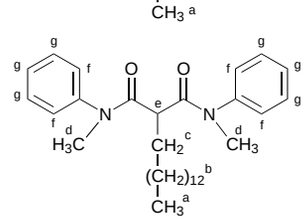	0.86–0.90 (3 H, t, a) 1.00–1.30 (24 H, m, b) 1.66–1.72 (2 H, q, c) 3.18 (6 H, s, d) 3.23–3.27 (1 H, t, e) 6.70 (4 H, m, f) 7.34 (6 H, m, g)

SHELXL 93.[16] All calculations were carried out on a Silicon Graphics R4000 Workstation at the University of Reading.

Atomic coordinates, thermal parameters and bond lengths and angles have been deposited at the Cambridge Crystallographic Data Centre (CCDC). See Instructions for Authors, *J. Chem. Soc., Dalton Trans.*, 1997, Issue 1. Any request to the CCDC for this material should quote the full literature citation and the reference number 186/333.

Results and Discussion

Metal extraction

Extraction data for some trivalent metals were determined with dmptdma and dcmtdma and compared with the data for uranium(VI) and thorium(IV) and the same trivalent metals extracted by dbmodma, Fig. 1. The extraction of metals at high nitric acid concentration (>7 mol dm^{-3} HNO_3) by dmptdma showed a constant increase which cannot be seen with either dbmodma or dcmtdma, both of which reach maxima at *ca.* 7 mol dm^{-3} HNO_3. It is believed that when the nitric acid concentrations are below 1 mol dm^{-3} the malonamide species (L) exists in the unprotonated form. Between acid concentrations of 1 and 6 mol dm^{-3} the dominant species is the monoprotonated $HL^+NO_3^-$, while the diprotonated form H_2L^{2+} $2NO_3^-$ is then thought to predominate above 7 mol dm^{-3} HNO_3.[17] The extraction of nitric acid supports this observation (Fig. 2). The extraction data in Fig. 1 indicate a point of inflection at *ca.* 1 mol dm^{-3} HNO_3, suggesting a change in extraction mechanism, which may be related to the malonamide species. For trivalent metal ions, from 1 to 6 mol dm^{-3} nitric acid the dominating species could be $HL^+M(NO_3)_4^-$. When the nitric acid concentration increases to 7 mmol dm^{-3} and above the extracting species becomes the diprotonated H_2L^{2+}. After L is diprotonated the extracted anion could be in the form of two $M(NO_3)_4^-$ anions or one $M(NO_3)_5^{2-}$ dianion. In order to extract these anions the protonated carbonyl groups must be available and it would appear that the diphenyl derivative can be protonated more readily than the other two malonamides. The different extraction mechanisms for trivalent metal ions by malonamides can thus be described as in equations (1)–(3) (L = malonamide).

Co-ordination mechanism

$$M^{3+} + 3NO_3^- + nL \rightleftharpoons M(NO_3)_3L_n \quad (\leqslant 1 \text{ mol dm}^{-3}\ HNO_3) \quad (1)$$

Ion-pair mechanism

$$HL^+ + M(NO_3)_4^- \rightleftharpoons HL^+M(NO_3)_4^- \quad (1 \leqslant [HNO_3] \leqslant 6 \text{ mol dm}^{-3}) \quad (2)$$

$$H_2L^{2+} + M(NO_3)_5^{2-} \rightleftharpoons H_2L^{2+}M(NO_3)_5^{2-} \quad (\geqslant 6 \text{ mol dm}^{-3}\ HNO_3) \quad (3)$$

Determination of the number of malonamide molecules

The number of malonamide molecules in the extracted species can be determined if the distribution ratio (*D*) for the metal extraction at a constant pH is plotted as a function of malonamide concentration; the slope is approximately equal to the number of malonamide molecules. (The distribution ratio is defined as the concentration of the metal species in the organic phase divided by its concentration in the aqueous phase.) Table 3 shows that there are between two and four malonamide molecules per metal ion, consistent with a co-ordination mechanism but not with an ion-pair mechanism. The discrepancy arising from conventional slope analysis often results in non-integral slopes for amide extractants. This is possibly due to the non-ideality of the organic solution or the presence of extra amide molecules in the second co-ordination sphere.[5] The result also reflects the possible aggregation of L/HNO_3 solvates in the organic phase (micelle formation).[18]

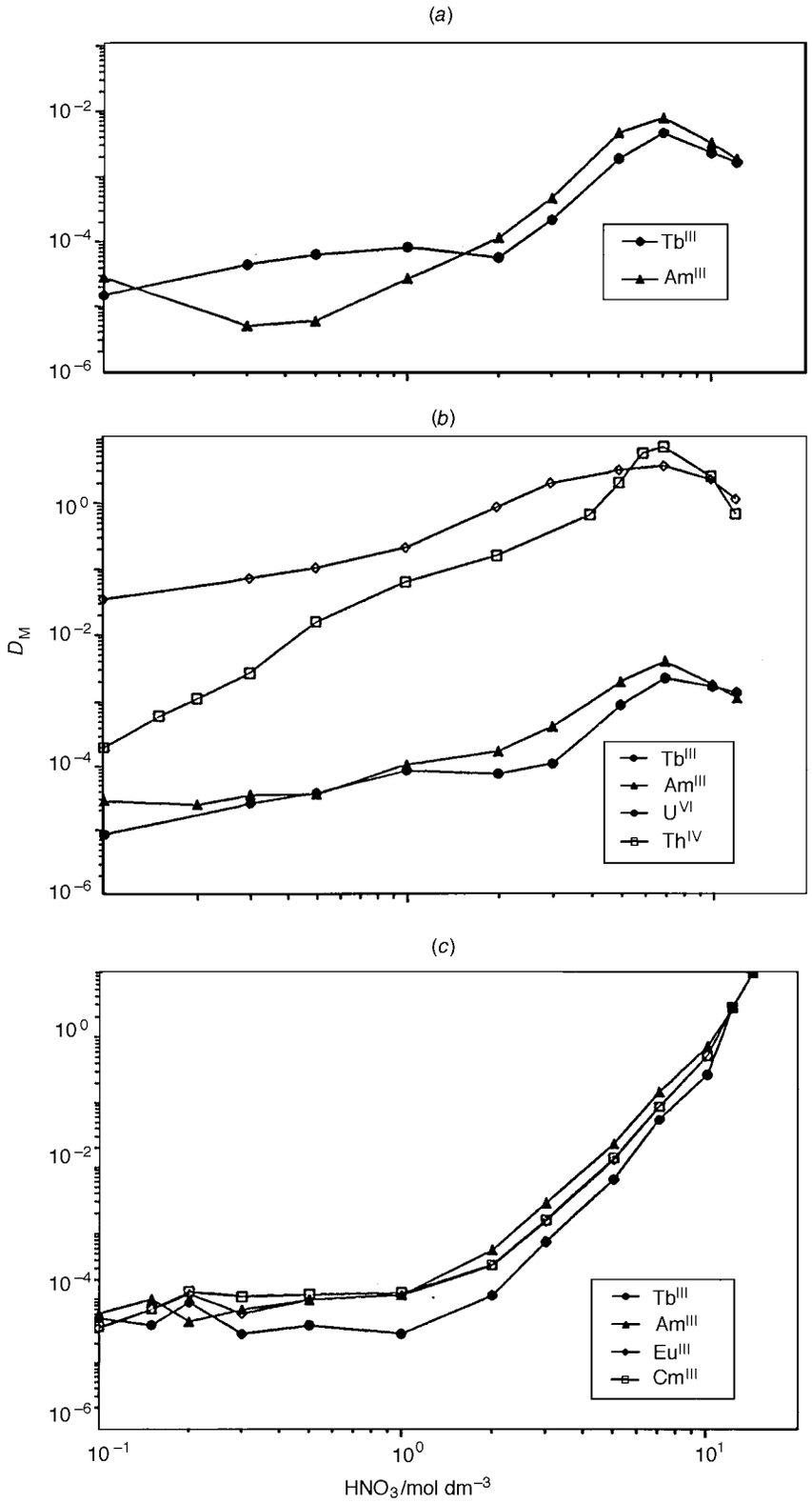

Fig. 1 Plots of the distribution coefficient *D vs.* nitric acid concentration for extractions by dcmtdma (*a*), dbmodma (*b*) and dmptdma (*c*)

Nitric acid extraction

The extent of nitric acid extraction does not show any significant difference between the two extractants dmptdma and dbmodma (Fig. 2). The number of nitric acid molecules extracted per malonamide increases uniformly with the nitric acid concentration. At 6 mol dm^{-3} HNO_3 the ratio between HNO_3 and the malonamides is approximately one for both extractants; when the nitric acid concentration reaches 7 mol dm^{-3} the ratio is between one and two. These values suggested that, in 5 mol dm^{-3} nitric acid, the dominating species is the monoprotonated form, $HL^{+}NO_3^{-}$, but in 7 mol dm^{-3} nitric acid the diprotonated form $H_2L^{2+}(NO_3)_2^{2-}$ predominates. These observations support the existence of an ion-pair mechanism involving either the mono- or di-protonated forms.

Table 3 Results of slope analysis for Am at 0.2–1 mol dm^{-3} malonamide

Malonamide	$[HNO_3]$/mol dm^{-3}	Slope	*r*	$[HNO_3]$/mol dm^{-3}	Slope	*r*
dbmodma	0.3	2.5	0.9940	3	2.3	0.9937
dmptdma	0.5	2.6	0.9835	2	2.7	0.9992
dcmtdma	1	3.6	0.9916	7.5	2.2	0.9979

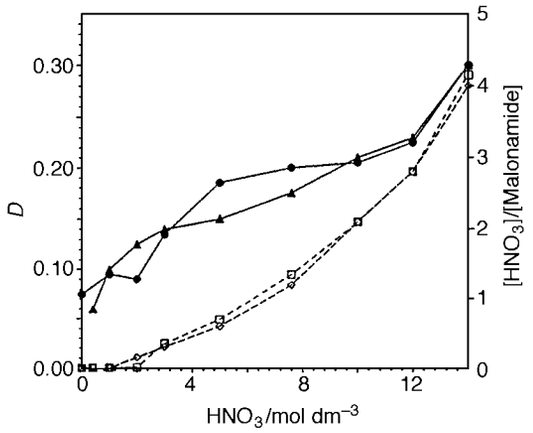

Fig. 2 Extraction of nitric acid by 0.1 mol dm^{-3} dbmodma in *tert*-butylbenzene (▲), by 0.1 mol dm^{-3} dmptdma in *tert*-butylbenzene (●) (both continuous lines, left scale) and the average number of HNO_3 molecules extracted per dbmodma molecule (◇) and per dmptdma molecule (□) (both dotted lines, right scale)

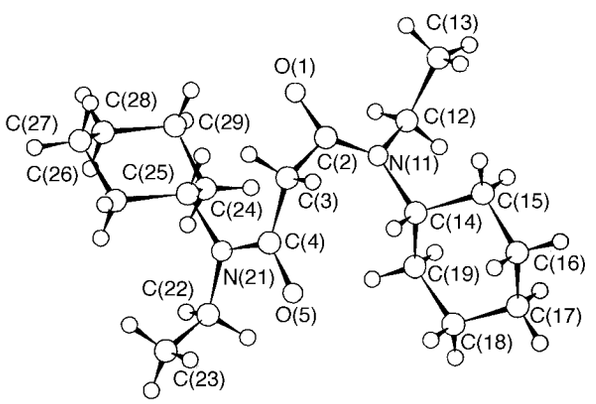

Fig. 3 Crystal structure of dcema showing the atomic numbering scheme

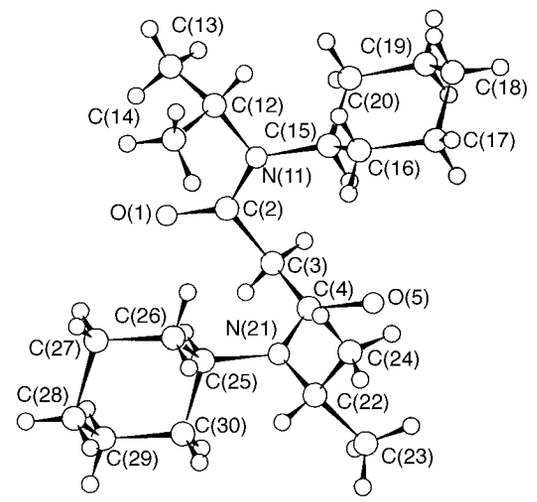

Fig. 4 Crystal structure of dcima showing the atomic numbering scheme

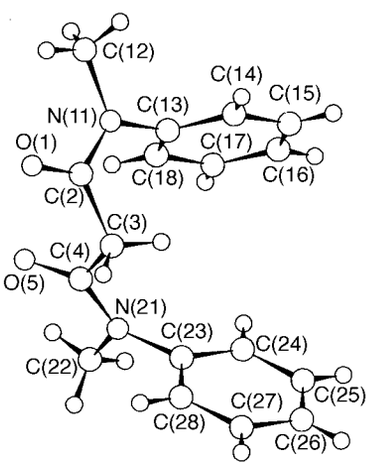

Fig. 5 Crystal structure of dmpma showing the atomic numbering scheme

Crystal structures

The structures are shown in Figs. 3–9 together with the atomic numbering schemes. The malonamide moieties are numbered in identical fashion in the seven structures.

Ligand conformations. The conformation of the malonamides can be described by the torsion angles listed in Table 4. These are the four torsion angles along the backbone from one acyclic carbon atom to the other [*e.g.* C(acyclic)–N–C–C, N–C–C–C, C–C–C–N and C–C–N–C (acyclic)]. In addition, the O(1)–C(2)···C(4)–O(5) torsion angles and O(1)···O(5) distances are listed. The conformations of dcema and dcima are very similar with a tggt (t = *trans*, g = *gauche*) pattern along the backbone and an overall *trans* conformation for O=C···C=O with the torsion angle being close to 180°. Both molecules exhibit approximate C_2 symmetry with the rotation axis passing through the central carbon atom C(3). The carbonyl group is *cis* to the acyclic groups on the nitrogen and *trans* to the bulkier cyclohexane group. The O···O distances are 4.44 and 4.48 Å respectively. By contrast in dmpma the backbone shows a ttgt pattern with an overall O=C···C=O torsion angle of 57.2° and an O···O distance of 3.29 Å. Clearly there is a major difference between the conformations with R = cyclohexyl and R = phenyl. The compound $Hdcmma^+$ contains two discrete

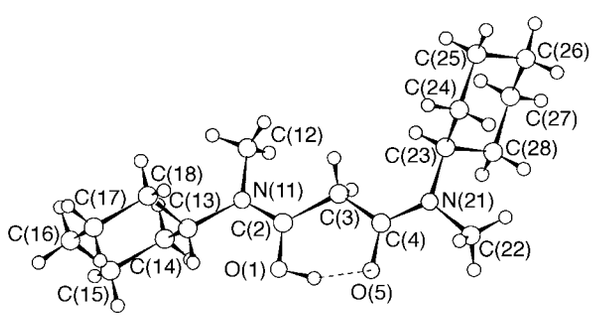

Fig. 6 Crystal structure of $Hdcmma^+$ showing the atomic numbering scheme. There are two cations in the asymmetric unit with similar geometries. Only one cation is shown. The hydrogen bond is shown as a dotted line

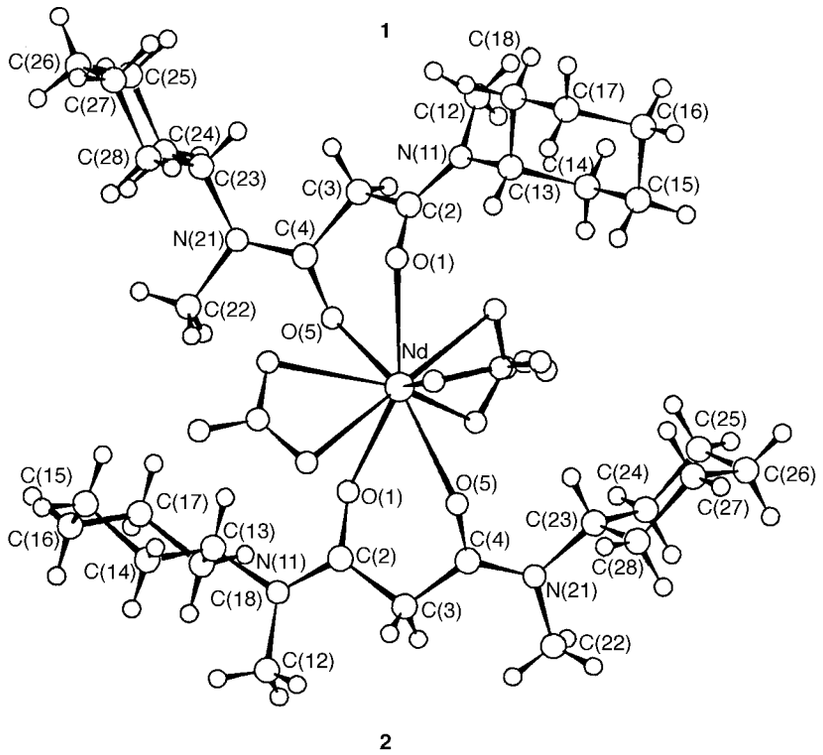

Fig. 7 Crystal structure of $[Nd(NO_3)_3(dcmma)_2]$ showing the atomic numbering scheme

cationic units together with a $[CoCl_4]^{2-}$ anion. The two cations (denoted A and B) have very similar geometries. For both cations it proved possible to locate the hydrogen atom bonded to O(1) and as is apparent from Fig. 6 this atom forms an intramolecular hydrogen bond to O(5). The O(1)···O(5), H(1)···O(5) and O(1)–H(1)···O(5) dimensions are 2.39, 1.45 Å, 165° in A and 2.40, 1.56 Å, 144° in B. For these cations the formation of the hydrogen bonds leads to a planar arrangement of the backbone with O(1)–C(2)···C(4)–O(5) torsion angles of 1.9° in A and 2.3° in B. The overall backbone pattern however is cggt and as shown in Fig. 6 the alkyl groups are arranged differently at the two ends of the malonamide. Thus at one end the cyclohexyl group is *trans* to the carbonyl and at the other the methyl group is *trans*. It is not clear why this should be but it is noteworthy that this conformation is found in the two independent cations. It is also significant that in both cations it is the carbonyl group *trans* to the methyl group that is protonated rather than the other carbonyl which is *trans* to the cyclohexyl group.

A search of the Cambridge Crystallographic Database[19] revealed seven structures containing the malonamide moiety and the O=C···C=O torsion angles all range between 66.2 and 115.9° with none being close to 180° (or less surprisingly 0°). Some of these structures have special features like substitution on the central carbon atom C(3) or internal hydrogen bonds which may cause this torsion angle to have a specific value but this is not true of all of them. While we have established a significant difference between the cyclohexyl and phenyl structures that is consistent with the different extraction properties of the two types of malonamide, it is not obvious why they should have different structures. We therefore investigated malonamide conformations using both molecular mechanics and quantum mechanics methods.

We first used the QUANTA/CHARMm package[20] for conformational analysis. Molecular dynamics was employed, heating the molecule up to 3000 K. The time step was 1 fs and after equilibration 1000 structures were saved at 100 fs intervals. These structures were then minimised and analysed. The crystal structures of dmpma and dcema were used as starting models, although in the latter the ethyl group was replaced by a methyl group to give the dimethyl analogue dcmma. For both structures many different conformations were obtained but only the four lowest-energy ones for each are shown in Table 4. Note that in both cases the lowest-energy conformation is similar to that found in the crystal structures, thus dmpma has the ttgt backbone with an O=C···C=O torsion angle of −70.4° and dcmma has the tggt backbone with an O=C···C=O torsion angle of 161.2°. It is clear from the molecular mechanics calculations that this difference is due to a large number of small energy terms rather than a few large terms. For dmpma the other three low-energy conformations all show much larger O···O distances. The third lowest-energy conformation has a similar conformation to that observed in dcmma. By contrast in dcmma the three lowest-energy conformations are tggt, tggc and cggc, thus all having similar *gauche-gauche* arrangements around the central N–C–C–C and C–C–C–N bonds but different arrangements of the methyl and cyclohexyl groups relative to the backbone. The fourth lowest-energy conformation is ttgt, equivalent to that found for the lowest energy of dmpma.

To confirm these energy preferences, particularly as the energy differences are small and the force field imperfect, we also carried out quantum-mechanics calculations on these eight lowest-energy conformations. Using the GAUSSIAN 94 program,[21] the geometries were those obtained from the refinement following the conformational analysis. The 6-31* basis set was used. The results confirm the conformational preferences found by the molecular mechanics calculations and the energies are listed in Table 4. The GAUSSIAN 94 program was also used to investigate the structure of the malonamide cation found in $Hdcmma^+$. Single-point calculations confirm the stability of the cation with the intramolecular hydrogen bond compared to an alternative structure with the hydrogen atom pointing away from the second oxygen atom which could lead to intermolecular hydrogen bonding. Respective energies were −920.240 and −920.214 hartree.

Metal complexes. The structures of the three complexes all contain malonamide acting as a bidentate ligand to a lanthanide metal. Bond lengths in the metal co-ordination spheres are listed in Tables 5–7. Torsion angles illustrating the malonamide

Table 4 Experimental and theoretical conformations of malonamides

(*a*) Experimental: torsion angles (°), distances (Å)

				Hdcmma^{+} [a]		[Nd(NO$_3$)$_3$(dcmma)$_2$] [b]		[Nd(NO$_3$)$_3$(H$_2$O)$_2$(dmpma)] [a]		
	dcema	dcima	dmpma	A	B	1	2	A	B	[Yb(NO$_3$)$_3$(H$_2$O)(dmpma)]
C(acyclic)–N(11)–C(2)–C(3)	176.8	−177.7	−177.4	2.2	0.1	−4.5	−13.2	−173.9	−172.8	178.9
N(11)–C(2)–C(3)–C(4)	−66.6	67.5	156.6	172.8	174.4	174.7	−132.0	−147.9	−149.3	145.7
C(2)–C(3)–C(4)–N(11)	−67.1	68.3	−84.8	−176.1	−172.8	136.4	−173.3	118.1	119.6	−119.8
C(3)–C(4)–N(21)–C(acyclic)	174.0	−176.9	−178.4	−175.0	−176.6	−179.2	2.2	−172.4	−174.6	168.0
O(1)–C(2) · · · C(4)–O(5)	−177.2	−177.1	57.2	1.9	2.3	−52.1	51.4	−20.2	−20.5	14.0
O(1) · · · O(5)	4.44	4.48	3.29	2.39	2.40	2.83	2.80	2.82	2.83	2.80

(*b*) Conformations with the four lowest energies as calculated by molecular mechanics

	dmpma				dcmma			
	1	2	3	4	1	2	3	4
C(Me)–N–C–C	−179.6	179.7	177.9	−179.1	−176.0	−176.4	2.1	170.7
N–C–C–C	74.0	−99.8	−59.4	74.1	59.9	62.3	63.4	−151.8
C–C–C–N	−159.9	−99.8	−59.4	61.1	59.9	60.0	63.4	65.6
C–C–N–C (Me)	179.1	179.7	177.9	2.1	−176.0	4.1	2.1	−177.4
O=C–C=O	−70.4	132.7	−158.0	174.4	161.2	164.4	168.5	−71.0
O · · · O	3.56	4.02	4.63	4.53	4.58	4.56	4.54	3.60
E/kcal mol^{-1}	8.16	8.99	9.70	11.05	13.17	13.76	14.54	17.10

(*c*) Energies (hartrees) of conformations calculated with GAUSSIAN 94

	Conformation			
Malonamide	1	2	3	4
dmpma	−912.898	−912.894	−912.891	−912.889
dcmma	−919.899	−919.898	−919.898	−919.894

[a] Two ligands in different structures. [b] Two ligands in the same structure.

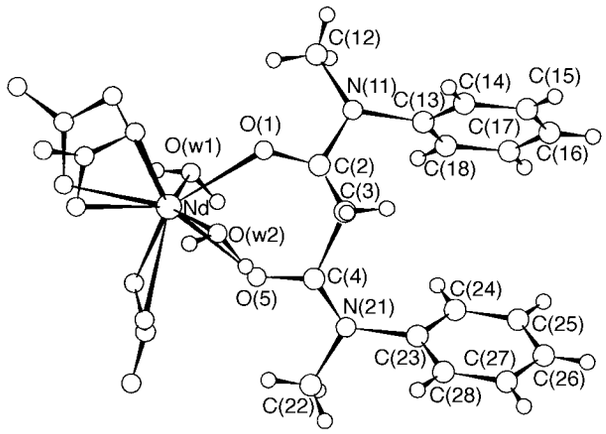

Fig. 8 Crystal structure of $[Nd(NO_3)_3(H_2O)_2(dmpma)]$ showing the atomic numbering scheme. There are two molecules in the asymmetric unit with similar geometries. Molecule A is shown

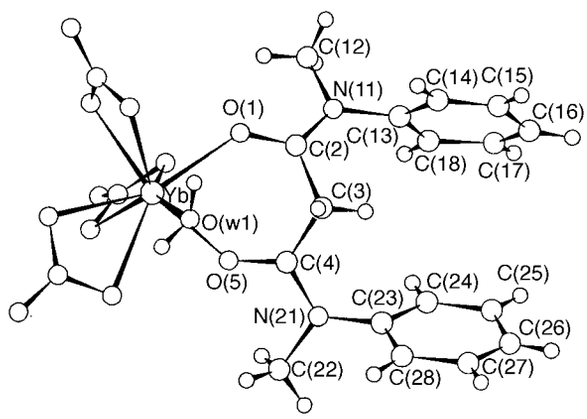

Fig. 9 Crystal structure of $[Yb(NO_3)_3(H_2O)(dmpma)]$ showing the atomic numbering scheme

conformation are given in Table 4. The structure of $[Nd(NO_3)_3(dcmma)_2]$ is shown in Fig. 7. The metal atom is ten-co-ordinate being bonded in a bidentate fashion to three nitrates and two malonamides. As is apparent from the figure, the malonamides are on opposite sides of the metal, with the nitrate ions fitted in an equatorial girdle. The bond lengths to the malonamide oxygen atoms at 2.46(1)–2.51(1) Å are shorter than those to the nitrate oxygen atoms [2.55(2)–2.82(2) Å]. A previous structure determination of $[La(NO_3)_3(tema)_2]$ (tema = *N*,*N*,*N*′-tetraethylmalonamide) had been carried out with $R^1 = R^2 = Et$.[22] While not isomorphous, the structures are very similar. There are two other known structures containing lanthanides and malonamides, *viz*. $[M(tema)_4][PF_6]_3$ (M = Sm or Er). Here the lanthanides are eight-co-ordinated being bonded to four bidentate ligands.[23]

The conformation of the malonamide ligand is somewhat surprisingly significantly non-planar with O=C···C=O torsion angles of −52.1 and 51.4° in the two ligands. The backbones are tttc and cttc, but with one angle of the central two angles differing significantly from the ideal at 136.4 and −132.0° in the two ligands. It is interesting that the ligands are also not planar in $[La(NO_3)_3(tema)_2]$ with torsion angles of 48.0 and −54.2°. Even in the tetramalonamide structures[23] two of the ligands are significantly non-planar (−32.0, −32.0°) while the other two are approximately planar at 1.6 and 1.6°. One unexpected feature of $[Nd(NO_3)_3(dcmma)_2]$ is that in one ligand the methyl groups are in different positions relative to its backbone, one being *cis* and the other *trans*. This asymmetric conformation was also found in the cation $Hdcmma^+$. However, in the other ligand the cttc arrangement is found.

Table 5 Geometry (distances in Å, angles in °) of the metal co-ordination sphere in $[Nd(NO_3)_3(dcmma)_2]$

Nd–O(11)	2.462(10)	Nd–O(202)	2.573(13)
Nd–O(21)	2.476(9)	Nd–O(201)	2.630(12)
Nd–O(15)	2.490(9)	Nd–O(102)	2.641(13)
Nd–O(25)	2.512(10)	Nd–O(103)	2.685(13)
Nd–O(301)	2.547(13)	Nd–O(302)	2.82(2)
O(11)–Nd–O(21)	147.9(3)	O(15)–Nd–O(102)	74.1(4)
O(11)–Nd–O(15)	69.7(3)	O(25)–Nd–O(102)	87.1(4)
O(21)–Nd–O(15)	141.6(3)	O(301)–Nd–O(102)	145.1(5)
O(11)–Nd–O(25)	81.8(3)	O(202)–Nd–O(102)	84.4(5)
O(21)–Nd–O(25)	68.4(3)	O(201)–Nd–O(102)	130.0(5)
O(15)–Nd–O(25)	149.7(3)	O(11)–Nd–O(103)	109.1(4)
O(11)–Nd–O(301)	83.0(4)	O(21)–Nd–O(103)	71.3(4)
O(21)–Nd–O(301)	75.0(4)	O(15)–Nd–O(103)	110.9(4)
O(15)–Nd–O(301)	117.3(4)	O(25)–Nd–O(103)	68.6(4)
O(25)–Nd–O(301)	67.1(4)	O(301)–Nd–O(103)	131.5(4)
O(11)–Nd–O(202)	139.8(4)	O(202)–Nd–O(103)	69.0(5)
O(21)–Nd–O(202)	71.6(4)	O(201)–Nd–O(103)	114.8(5)
O(15)–Nd–O(202)	73.8(4)	O(102)–Nd–O(103)	46.8(4)
O(25)–Nd–O(202)	128.6(4)	O(11)–Nd–O(302)	69.6(4)
O(301)–Nd–O(202)	129.8(5)	O(21)–Nd–O(302)	108.9(4)
O(11)–Nd–O(201)	130.7(4)	O(15)–Nd–O(302)	70.3(4)
O(21)–Nd–O(201)	70.5(4)	O(25)–Nd–O(302)	109.5(4)
O(15)–Nd–O(201)	74.6(4)	O(301)–Nd–O(302)	47.2(4)
O(25)–Nd–O(201)	134.5(4)	O(202)–Nd–O(302)	113.0(5)
O(301)–Nd–O(201)	84.4(5)	O(201)–Nd–O(302)	67.0(5)
O(202)–Nd–O(201)	49.7(5)	O(102)–Nd–O(302)	133.0(4)
O(11)–Nd–O(102)	69.9(4)	O(103)–Nd–O(302)	178.0(5)
O(21)–Nd–O(102)	118.0(4)		

Structures $[Nd(NO_3)_3(H_2O)_2(dmpma)]$ and $[Yb(NO_3)_3(H_2O)(dmpma)]$ are shown in Figs. 8 and 9. Both contain only one dmpma ligand rather than two. In the case of the neodymium complex, several attempts were made to prepare complexes, each time using different metal : ligand ratios, but with ratios of 3 : 1, 2 : 1, 1 : 1 and 1 : 2 the 1 : 1 complex precipitated in each case (yields *ca.* 50%). A Fourier-transform IR study of extracted lanthanide malonamide species in benzene suggested that the solutions consisted of a mixture containing complexes with both one and two malonamide ligands. The nature of these spectra suggested, however, that both complexes were anhydrous.[24] It seems likely that if both complexes are formed in solution the solubility of each in the chosen solvent determines which precipitates. The complex $[Nd(NO_3)_3(H_2O)_2(dmpma)]$ contains ten-co-ordinated neodymium bonded to three nitrates, the malonamide and two water molecules, while $[Yb(NO_3)_3(H_2O)(dmpma)]$ contains nine-co-ordinated ytterbium, three nitrates, the malonamide, but only one water molecule. The difference in stoichiometry is probably due to the differing sizes of the two metals, Nd being an early lanthanide with a larger radius and Yb a late lanthanide with a smaller radius. There are two molecules in the asymmetric unit for the neodymium complex, but both have similar dimensions. In both cases the bond lengths are approximately in the sequence Nd–O (malonamide) < Nd–O (water) < Nd–O (nitrate) with distances in the ranges 2.40(1)–2.49(1), 2.54(1)–2.59(1) and 2.58(1)–2.69(1) Å respectively. For the ytterbium complex the same order pertains but with much shorter distances, Yb–O (malonamide) 2.27(1)–2.30(1), Yb–O (water) 2.35(1) and Yb–O (nitrate) 2.40(1)–2.48(1) Å. It is interesting that, for these structures containing just one malonamide ligand, the conformation is more closely planar with O=C···C=O torsion angles of (−20.5, −20.2°) and 14.0° respectively. In both cases, however, the arrangement of the ligands is similar in that the carbonyl

Table 6 Bond lengths (Å) and angles (°) for $[Nd(NO_3)_3(H_2O)_2(dmpma)]$

Molecule A		Molecule B	
Nd(1)–O(5)	2.428(8)	Nd(2)–O(5)	2.398(7)
Nd(1)–O(1)	2.477(8)	Nd(2)–O(1)	2.490(8)
Nd(1)–O(w1)	2.541(9)	Nd(2)–O(61)	2.575(8)
Nd(1)–O(w2)	2.580(9)	Nd(2)–O(w1)	2.581(9)
Nd(1)–O(71)	2.595(8)	Nd(2)–O(w2)	2.594(9)
Nd(1)–O(52)	2.600(9)	Nd(2)–O(72)	2.617(9)
Nd(1)–O(51)	2.610(9)	Nd(2)–O(51)	2.618(9)
Nd(1)–O(62)	2.617(9)	Nd(2)–O(53)	2.637(9)
Nd(1)–O(72)	2.630(9)	Nd(2)–O(62)	2.672(10)
Nd(1)–O(61)	2.669(9)	Nd(2)–O(71)	2.688(8)
O(5)–Nd(1)–O(1)	70.4(3)	O(5)–Nd(2)–O(1)	70.0(3)
O(5)–Nd(1)–O(w1)	76.5(3)	O(5)–Nd(2)–O(61)	77.6(3)
O(1)–Nd(1)–O(w1)	74.9(3)	O(1)–Nd(2)–O(61)	131.4(3)
O(5)–Nd(1)–O(w2)	80.9(3)	O(5)–Nd(2)–O(w1)	80.1(4)
O(1)–Nd(1)–O(w2)	72.4(3)	O(1)–Nd(2)–O(w1)	70.2(4)
O(w1)–Nd(1)–O(w2)	144.9(5)	O(61)–Nd(2)–O(w1)	69.3(3)
O(5)–Nd(1)–O(71)	77.2(3)	O(5)–Nd(2)–O(w2)	75.9(3)
O(1)–Nd(1)–O(71)	131.1(3)	O(1)–Nd(2)–O(w2)	74.6(4)
O(w1)–Nd(1)–O(71)	131.2(2)	O(61)–Nd(2)–O(w2)	130.9(3)
O(w2)–Nd(1)–O(71)	67.1(3)	O(w1)–Nd(2)–O(w2)	142.5(6)
O(5)–Nd(1)–O(52)	139.1(3)	O(5)–Nd(2)–O(72)	119.1(3)
O(1)–Nd(1)–O(52)	80.4(3)	O(1)–Nd(2)–O(72)	148.0(3)
O(w1)–Nd(1)–O(52)	68.5(3)	O(61)–Nd(2)–O(72)	79.7(3)
O(w2)–Nd(1)–O(52)	117.2(3)	O(w1)–Nd(2)–O(72)	139.2(4)
O(31)–Nd(1)–O(52)	142.9(3)	O(w2)–Nd(2)–O(72)	78.2(4)
O(5)–Nd(1)–O(51)	138.2(3)	O(5)–Nd(2)–O(51)	139.7(3)
O(1)–Nd(1)–O(51)	73.9(3)	O(1)–Nd(2)–O(51)	81.7(3)
O(w1)–Nd(1)–O(51)	114.4(3)	O(61)–Nd(2)–O(51)	141.5(3)
O(w2)–Nd(1)–O(51)	67.9(3)	O(w1)–Nd(2)–O(51)	117.1(3)
O(71)–Nd(1)–O(51)	112.7(3)	O(w2)–Nd(2)–O(51)	69.1(3)
O(52)–Nd(1)–O(51)	50.3(3)	O(72)–Nd(2)–O(51)	73.0(4)
O(5)–Nd(1)–O(62)	120.9(3)	O(5)–Nd(2)–O(53)	139.1(3)
O(1)–Nd(1)–O(62)	147.1(3)	O(1)–Nd(2)–O(53)	74.9(3)
O(w1)–Nd(1)–O(62)	78.2(4)	O(61)–Nd(2)–O(53)	113.0(3)
O(w2)–Nd(1)–O(62)	136.9(4)	O(w1)–Nd(2)–O(53)	68.7(3)
O(71)–Nd(1)–O(62)	81.3(3)	O(w2)–Nd(2)–O(53)	114.1(2)
O(52)–Nd(1)–O(62)	72.3(4)	O(72)–Nd(2)–O(53)	101.8(3)
O(51)–Nd(1)–O(62)	100.9(3)	O(51)–Nd(2)–O(53)	49.7(3)
O(5)–Nd(1)–O(72)	125.1(3)	O(5)–Nd(2)–O(62)	126.1(3)
O(1)–Nd(1)–O(72)	134.4(3)	O(1)–Nd(2)–O(62)	135.2(3)
O(w1)–Nd(1)–O(72)	145.6(4)	O(61)–Nd(2)–O(62)	49.7(3)
O(w2)–Nd(1)–O(72)	69.4(4)	O(w1)–Nd(2)–O(62)	72.4(4)
O(71)–Nd(1)–O(72)	49.2(3)	O(w2)–Nd(2)–O(62)	145.0(4)
O(52)–Nd(1)–O(72)	95.8(3)	O(72)–Nd(2)–O(62)	67.3(3)
O(51)–Nd(1)–O(72)	69.4(3)	O(51)–Nd(2)–O(62)	94.2(3)
O(62)–Nd(1)–O(72)	67.7(3)	O(53)–Nd(2)–O(62)	69.1(3)
O(5)–Nd(1)–O(61)	72.7(3)	O(5)–Nd(2)–O(71)	70.5(3)
O(1)–Nd(1)–O(61)	130.4(3)	O(1)–Nd(2)–O(71)	128.8(3)
O(w1)–Nd(1)–O(61)	65.0(3)	O(61)–Nd(2)–O(71)	67.3(3)
O(w2)–Nd(1)–O(61)	132.0(3)	O(w1)–Nd(2)–O(71)	131.6(3)
O(71)–Nd(1)–O(61)	68.3(3)	O(w2)–Nd(2)–O(71)	65.1(3)
O(52)–Nd(1)–O(61)	108.9(3)	O(72)–Nd(2)–O(71)	48.5(3)
O(51)–Nd(1)–O(61)	149.1(3)	O(51)–Nd(2)–O(71)	110.1(3)
O(62)–Nd(1)–O(61)	48.2(3)	O(53)–Nd(2)–O(71)	150.3(3)
O(72)–Nd(1)–O(61)	94.1(3)	O(62)–Nd(2)–O(71)	94.7(3)

groups are *cis* to the methyl groups and *trans* to the phenyl rings.

Thus with the dicyclohexyl ligand we can only isolate complexes with two malonamides, while with the diphenyl ligand we can only isolate complexes with one malonamide. Clearly the preparation (or not) of crystals is not definite evidence of a significant difference between the complexation properties of the two ligands. However, we have also reported here two further pieces of evidence indicating different behaviour. First our experimental and computational structural studies have shown that the cyclohexyl compound is likely to have the *trans* O=C···C=O conformation while the phenyl has the *gauche*. Secondly our extraction studies also show a significant difference in that the diphenyl compound is far more successful at extraction than is the dicyclohexyl.

Table 7 Distances (Å) and angles (°) in the metal co-ordination sphere of $[Yb(NO_3)_3(H_2O)(dmpma)]$

Yb–O(1)	2.274(6)	Yb–O(51)	2.460(8)
Yb–O(5)	2.296(8)	Yb–O(61)	2.474(9)
Yb–O(300)	2.350(8)	Yb–O(53)	2.473(7)
Yb–O(62)	2.396(8)	Yb–O(71)	2.481(8)
Yb–O(73)	2.447(8)		
O(1)–Yb–O(5)	75.8(3)	O(62)–Yb–O(61)	53.5(3)
O(1)–Yb–O(300)	77.7(3)	O(73)–Yb–O(61)	72.3(3)
O(5)–Yb–O(300)	84.3(3)	O(51)–Yb–O(61)	121.6(3)
O(1)–Yb–O(62)	91.4(3)	O(1)–Yb–O(53)	73.8(3)
O(5)–Yb–O(62)	125.9(3)	O(5)–Yb–O(53)	144.8(2)
O(300)–Yb–O(62)	144.7(3)	O(300)–Yb–O(53)	72.3(3)
O(1)–Yb–O(73)	153.1(3)	O(62)–Yb–O(53)	72.4(3)
O(5)–Yb–O(73)	89.7(3)	O(73)–Yb–O(53)	125.1(3)
O(300)–Yb–O(73)	123.9(3)	O(51)–Yb–O(53)	52.8(2)
O(62)–Yb–O(73)	78.8(3)	O(61)–Yb–O(53)	119.4(3)
O(1)–Yb–O(51)	126.6(2)	O(1)–Yb–O(71)	140.9(2)
O(5)–Yb–O(51)	152.7(3)	O(5)–Yb–O(71)	77.2(3)
O(300)–Yb–O(51)	85.9(3)	O(300)–Yb–O(71)	71.8(2)
O(62)–Yb–O(51)	73.8(3)	O(62)–Yb–O(71)	127.5(3)
O(73)–Yb–O(51)	74.9(3)	O(73)–Yb–O(71)	52.5(3)
O(51)–Yb–O(61)	81.7(3)	O(51)–Yb–O(71)	75.5(3)
O(5)–Yb–O(61)	72.6(3)	O(61)–Yb–O(71)	116.1(3)
O(300)–Yb–O(61)	152.2(3)	O(53)–Yb–O(71)	117.7(2)

Conclusion

The use of malonamides for the coextraction of some trivalent lanthanides and actinides have been investigated. These malonamides proved to be readily prepared and the method is suitable for large-scale synthesis. Metal extraction increases as the nitric acid concentration increases for all three studied malonamides. The most important feature of the extraction was that points of inflection were observed for the distribution coefficients as a function of nitric acid concentration at about 1 and 6 mol dm^{-3}. The reasons for this can be related to changes in the mechanisms of extraction; for example, at low nitric acid concentrations ($\leqslant$1 mol dm^{-3}), a co-ordination mechanism dominates but as the acidities increase the ion-pair mechanism(s) are more important. These proposed mechanisms for metal extraction were supported by the crystal structures of $[Nd(NO_3)_3(dcmma)_2]$ for the co-ordination mechanism or $Hdcmma^+$ for the ion-pair mechanism involving a monoprotonated species. The first of these compounds was grown under neutral conditions which could represent the extracted species when the malonamide is not protonated. As acidities increase, malonamides become mono- or di-protonated at the carbonyl oxygen and the extracted metal species could be in their anionic form, *e.g.* $M(NO_3)_4^-$ or $M(NO_3)_5^{2-}$. The extent of nitric acid extraction by dmptdma and dbmodma showed that as the acidities increase above 1 mol dm^{-3} the number of nitric acid molecules extracted per malonamide was one and as the nitric acid concentration reached 5 mol dm^{-3} there were between one and two molecules extracted per malonamide. All of this evidence suggests that the mechanism of extraction of metals by malonamides depends upon the acidity of the medium: *i.e.* (1) a co-ordination mechanism at low acid concentrations and (2) an ion-pair mechanism at higher acid concentrations.

It was also interesting that the free malonamides dcema and dcima exist as *trans* conformers in which the carbonyl groups are lying mainly *trans* to each other. In order for the metals to form chelates with malonamides the carbonyl groups have to reorientate and lie *cis* to each other in order to facilitate extraction *via* either co-ordination or ion-pair mechanisms.

The diphenyl derivative dmpma on the other hand has a *gauche* arrangement of the two carbonyl groups and so the necessary reorientation is far less. This seems to be consistent with the fact that dmptdma is able to extract rare earths even at

Table 8 Crystal data for the seven structures

	dcema	dcima	dmpma	$[Hdcmma]_2[CoCl_4]$	$[Nd(NO_3)_3(dcmma)_2]$	$[Nd(NO_3)_3(H_2O)_2(dmpma)]$	$[Yb(NO_3)_3(H_2O)(dmpma)]$
Empirical formula	$C_{19}H_{34}N_2O_2$	$C_{21}H_{38}N_2O_2$	$C_{17}H_{18}N_2O_2$	$C_{34}H_{62}Cl_4CoN_4O_4$	$C_{34}H_{60}N_7NdO_{13}$	$C_{17}H_{22}N_5NdO_{13}$	$C_{17}H_{20}N_5O_{12}Yb$
M	322.48	350.53	282.33	791.35	919.13	640.6	659.42
Crystal system	Orthorhombic	Triclinic	Monoclinic	Monoclinic	Monoclinic	Orthorhombic	Monoclinic
Space group	*Pbca*	*P*$\bar{1}$	*C*2/*c*	$P2_1/c$	$P2_1/a$	$Pn2_1a$	$P2_1/n$
Unit cell dimensions							
a/Å	11.742(8)	9.390(7)	14.873(12)	13.543(13)	11.304(9)	21.480(12)	16.077(13)
b/Å	11.893(9)	11.517(10)	11.134(12)	23.568(18)	28.99(2)	26.705(14)	8.694(9)
c/Å	25.850(13)	11.326(10)	19.80(2)	14.468(13)	13.760(11)	8.992(8)	17.95(2)
α/°		100.7(1)					
β/°		106.8(1)	95.74(1)	111.11(1)	100.33(1)		97.07(1)
γ/°		112.9(1)					
U/Å^3	3610	1017	3262	4309	4436	5158	2490
Z	8	2	8	4	4	8	4
D_c/Mg m^{-3}	1.187	1.144	1.150	1.220	1.376	1.650	1.759
μ/mm^{-1}	0.076	0.073	0.076	0.683	1.231	2.085	3.826
F(000)	1424	388	1200	1684	1908	2552	1292
Crystal size/mm	0.4 × 0.35 × 0.3	0.35 × 0.35 × 0.4	0.3 × 0.3 × 0.35	0.3 × 0.25 × 0.30	0.25 × 0.25 × 0.30	0.15 × 0.20 × 0.25	0.25 × 0.25 × 0.40
θ range for collection/°	3.43–24.99	2.41–24.71	2.29–24.96	1.74–25.08	2.26–25.03	2.39–24.91	2.55–24.92
hkl Ranges	0–13, −10 to 8, −30 to 30	0–10, −13 to 12, −13 to 12	0–18, −12 to 12, −23 to 23	0–15, −27 to 27, −17 to 16	−12 to 12, 0–33, 0–16	−24 to 24, −30 to 30, 0–9	0–18, −10 to 10, −21 to 21
Reflections collected	6043	3125	4249	11 980	12 448	14 351	6256
Independent reflections	2380	3125	2498	6870	6863	8000	3897
R_{int}	0.038		0.042	0.045	0.0536	0.0369	0.0678
Weighting scheme* (*a*, *b*)	0.083, 0.978	0.342, 4.342	0.41, 12.35	0.511, 35.51	0.080, 287.99	0.068, 46.678	0.409, 12.35
Data restraints, parameters	2380, 0, 212	3125, 0, 236	2496, 0, 192	6870, 0, 442	6863, 0, 501	8000, 0, 654	3897, 0, 318
Goodness of fit on F^2	1.120	0.388	0.672	0.537	0.870	1.019	0.565
Final *R*1, *wR*2 indices [$I > 2\sigma(I)$]	0.0523, 0.1456	0.0525, 0.1772	0.0777, 0.1487	0.0928, 0.3060	0.0983, 0.2537	0.0488, 0.1320	0.0704, 0.2052
(all data)	0.0638, 0.1558	0.0643, 0.2020	0.1198, 0.2456	0.1488, 0.3946	0.1420, 0.2751	0.0596, 0.1467	0.0821, 0.2477
Largest difference peak and hole/e Å^{-3}	0.164, −0.157	0.173, −0.220	0.257, −0.362	1.035, −0.813	2.128, −1.865	1.458, −2.088	3.684, −3.587

* $w = 1/[\sigma^2(F_o^2) + (aP)^2 + bP]$, where $P = (F_o^2 + 2F_c^2)/3$.

the highest acid concentrations compared to dcmtdma and dbmodma where the extraction reaches a maximum at about 7 mol dm^{-3}, decreasing thereafter.

Acknowledgements

We are grateful for the financial support by the Swedish Nuclear and Waste Management Co., SKB and the European Union Nuclear Fission Safety Programme Task 2 (Contract F12W-CT91-0112). We are indebted to Pamela D. Chalmers, Mark R. Feaviour and Philip Turner for their help with the synthesis and preparation of crystals. We would also like to thank the EPSRC and The University of Reading for funding of the image-plate system.

References

1 J. Tommasi, M. Delpech, J. P. Grouiller and A. Zaetta, *Nucl. Technol.*, 1995, **111**, 133.
2 M. Salvatores, A. Zaetta, C. Girard, M. Delpech, I. Slessarev and J. Tommasi, *Int. J. Appl. Radiat. Isot.*, 1995, **46**, 681.
3 J. Emsley, *The Elements*, Clarendon Press, Oxford, 1989.
4 Z. Kolarik, *Separation of Actinides and Long-lived Fission Products from High-level Radioactive Wastes* (*a review*), Kernforschungszentrum, Karlsruhe, 1991.
5 C. Musikas and H. Hubert, *Ion Exch. Solvent Extr.*, 1987, **5**, 877.
6 G. F. Best, E. Hesford and H. A. C. McKay, *J. Inorg. Nucl. Chem.*, 1959, **12**, 136.
7 D. Scargill, K. Alcock, J. M. Fletcher, E. Hesford and H. A. C. McKay, *J. Inorg. Nucl. Chem.*, 1957, **4**, 304.
8 W. W. Schulz and E. P. Horwitz, *Sep. Sci. Technol.*, 1988, **23**, 1191.
9 E. P. Horwitz and W. W. Schulz, *Solvent Extraction and Ion Exchange in the Nuclear Fuel Cycle*, eds. D. H. Logsdail and A. L. Mills, Ellis Horwood, Chichester, 1985.
10 T. H. Siddall III, R. L. McDonald and W. E. Stewart, *J. Mol. Spectrosc.*, 1968, **28**, 243.
11 C. Musikas, *Inorg. Chim. Acta*, 1987, **140**, 197.
12 C. Cuillerdier, C. Musikas, P. Hoel, L. Nigond and X. Vitart, *Sep. Sci. Technol.*, 1991, **26**, 1229.
13 Q. Tian and M. A. Hughes, *Hydrometallurgy*, 1994, **36**, 79.
14 W. Kabsch, *J. Appl. Crystallogr.*, 1988, **21**, 916.
15 SHELXS 86, G. M. Sheldrick, *Acta Crystallogr., Sect. A*, 1990, **46**, 467.
16 SHELXL 93, G. M. Sheldrick, program for crystal structure refinement, University of Göttingen, 1993.
17 P. Byers and M. J. Hudson, unpublished work.
18 L. Nigond, N. Condamines, P. Y. Cordier, J. Livet, C. Madic, C. Cuillerdier, C. Musikas and M. J. Hudson, *Sep. Sci. Technol.*, 1995, **30**, 2075.
19 F. H. Allen and O. Kennard, *Chemical Design Automation News*, 1993, **8**, 31.
20 QUANTA/CHARMm, Version 3.23, Molecular Simulations Inc., Cambridge, UK; Waltham, MA, USA, 1996.
21 GAUSSIAN 94, Revision A.1, M. J. Frisch, G. W. Trucks, H. B. Schlegel, P. M. W. Gill, B. G. Johnson, M. A. Robb, J. R. Cheeseman, T. A. Keith, G. A. Petersson, J. A. Montgomery, K. Raghavachari, M. A. Al-Laham, V. G. Zakrzewski, J. V. Ortiz, J. B. Foresman, J. Cioslowski, B. B. Stefanov, A. Nanayakkara, M. Challalcombe, C. Y. Peng, P. Y. Ayala, W. Chen, M. W. Wong, J. L. Andres, E. S. Replogle, R. Gomperts, R. L. Martin, D. J. Fox, J. S. Binkley, D. J. Defrees, J. Baker, J. P. Stewart, M. Head-Gordon, C. Gonzalez and J. A. Pople, Gaussian Inc., Pittsburgh, PA, 1995.
22 P. Byers, M. G. B. Drew, M. J. Hudson, N. S. Isaacs and C. Madic, *Polyhedron*, 1994, **15**, 349.
23 E. E. Castellano and R. W. Becker, *Acta Crystallogr., Sect. B*, 1981, **37**, 61.
24 L. Nigond, Ph.D. Thesis, Université Blaise Pascal, 1992, CEA-R-5610.

Received 9*th August* 1996; *Paper* 6/05577J